AUTOMATED CRATER DETECTION AND COUNTING USING THE HOUGH TRANSFORM AND CANNY EDGE DETECTION. M. J. Galloway[1], J. Paxman[2], G. K. Benedix[3,*], T. Tan[2], M. C. Towner[3], and P. A. Bland[3], [1]Department of Mechanical Engineering, Curtin University, GPO Box U1987, Perth, WA 6845, Australia; [2]Department of Mechanical Engineering, Curtin University, GPO Box U1987, Perth, WA 6845, Australia; [3]Department of Applied Geology, Curtin University, GPO Box U1987, Perth, WA 6845, Australia. (*corresponding author: g.benedix@curtin.edu.au)

Introduction: Impact cratering is the most common geological process occurring in solar system, and it is used to estimate the ages of surfaces that have never been sampled and, thus, cannot be isotopically dated [1, 2]. In particular, densities of superposed craters are used to model crater ages in [3], however this is determined using a database of manually catalogued craters. Currently, the smallest craters recorded in the available databases are around 1km in diameter [2].

The resolution of images of the surface of Mars has increased by orders of magnitudes with recent orbiters. Cameras on board Mars Express (HRSC) and Mars Reconnaissance Orbiter (HiRISE) are mapping the surface of Mars at 10's cm/pixel [4,5] (compared with Viking orbiter data at 150-300 m/pixel). There are >35,000 images at this resolution. This is an unprecedented amount of data. We can now see craters on Mars meters in diameter. There is the potential here to determine surface ages at extremely high resolution. The primary obstacle is data reduction. A combination of these data will provide an opportunity to count craters down to sub-km sizes, giving unprecedented precision for ages of the surface features on Mars.

With smaller crater diameters comes an increase in frequency and consequently a significant increase in time required to identify such geological features, rendering the process impractical for surveys covering large surface areas. Thus there is a need for a system which can identify sub-km impacts automatically.

The potential of Crater Detection Algorithms (CDAs) and other automated approaches is huge [], but the main obstacle to general implementation is access to High Performance Computing. One study exploring automated crater counting reported a modest rate of 93μs/pixel on a dual Xeon processor workstation [6]. The tested CDA had reasonable performance (a reported detection rate of 70% [6]). For a single Mars Express HRSC image, with pixel dimensions of 11211 x 47509, this translates to ~14 hrs of desktop processing time, while a single high-resolution HiRISE image (with pixel dimensions 19582 x 67489) took 34hrs. There are >31,000 HiRISE images. What is required is access to a supercomputing facility.

The Square Kilometre Array (SKA) project coming to Western Australia has accelerated the development of supercomputing facilities such as iVEC's Pawsey Centre, which now includes the petascale supercomputer Magnus. There is a mandated 25% allocation for geoscience computing projects, which will provide the opportunity for applying the appropriate supercomputing resources this project, and its future work, require.

We report here on progress made so far in developing an automated system using a Hough Transform (HT) combined with Canny edge detection, with initial tests performed on HRSC images. Our approach also allows large scale automation of the work-flow in a parallel supercomputing environment.

Method: We extracted 15 regions of interest (ROI), each 2598 by 2664 pixels, from 5 HRSC images (h8304_0000, h0466_0000, h2530_0001, h9615_0000, and h7347_0000 [5, 7]) for our initial test data set. For each of these, craters >5 pixel radius were identified by visual inspection.

To test the performance of the automation algorithm requires a classification system that encapsulates a positive/negative test. Difficulty arises when attempting to test the outcomes True Positive (TP), False Positive (FP), False Negative (FN) and True Negative (TN). For example, one method may check for TPs, FPs, and FNs by comparing ground truth data with detection data. Defining a TN is more difficult, however, since every pixel in an image is a candidate for a crater center.

An alternative method to test the HT's performance is based on a set of candidate windows which have been manually classified as either positive or negative; they either contain a crater, or they do not. The evaluation of the classification system follows naturally.

Results: Performance of the HT was measured using a Receiver Operating Characteristic (ROC) curve (Figure 1). The *x*-axis represents the False Positive Rate (FPR), while the *y*-axis is the True Positive Rate (TPR). These metrics are similar to those used in [8], however we include the TN quantification.

The curve in Fig. 1 is parametric, with each point being representative of the performance at some varying sensitivity parameter within the edge detection scheme. The shape of an ROC curve is indicative of the detection algorithm's performance. Ideally, an ROC curve will include points (0, 0) for the lowest sensitivity parameter, (1, 1) for the highest (i.e. detect everything) and (0, 1) for some optimal parameter value.

Three sets of results were compared using ROC curves (Figure 1). Each curve represents different parameters used by the edge detection. By comparing these curves, we can infer whether and how much the edge detection or the HT's influences the algorithms performance. The detection performance using parameters from blue curve is illustrated in Figure 2.

The conclusion from Figure 1 is that the TPR can be increased with a higher amount of edge data. However, since decreasing the parameters for the edge detection increases the edge data uniformly across the image, we see a rise in FPR. This implies that an increase in edge data only around craters would be best.

Discussion and Future Work: An improvement to the edge detection stage under evaluation involves calculating image gradients in the direction of the solar azimuth angle (available from image metadata). This approach is expected to improve the performance of the edge detection stage since the visual features associated with craters are most often due to shadows and highlights, and hence typically perpendicular to the solar azimuth.

Currently the convolution kernels used for the sun direction gradient edge detection are only representative of north, south, east, west, and their combinatorial counterparts (e.g. north-east, south-east etc.). It will be possible to improve on this discretization once the metadata of HiRISE images are considered, since the sun direction can be calculated more precisely. This also makes it possible for the process to be automated.

Further developments will explore using the Hough Transform approach with suitably low thresholds as a prefilter for selecting candidate crater windows for a second stage, involving a Support Vector Machine or Neural Network.

The progress so far leaves the detection phase as completely automated. However, as of yet there have been no optimizations made or attempts to parallelize the algorithms or workflow. Due to the volume of data we anticipate processing, access to a supercomputing system will provide the opportunity to analyse more of it concurrently, and make processing of a large scale area practical. In addition, the algorithms offer themselves to parallelization. For example, the general HT may vote in the accumulator space at different radii in parallel, since each radius' voting space is independent. This too will be explored in future work.

References: [1] R.E. Arvidson, et al 1979. *Icarus*, 37, 467–474. [2] S.J. Robbins and B.M. Hynek, 2012 *J.G.R.*, 117 E05004, doi:10.1029/2011JE003966 [3] S.J. Robbins, et al. *Icarus*, 225, 173–184. [4] A. S. McEwen, et al., 2007. JGR Planets, 112, E05S02, doi:10.1029/2005JE002605 [5] R. Jaumann et al. 2007 *Planet. Space Sci.*, 55, 928–952.[6] E.R. Urbach and T.F. Stepinski 2009, *Planet. Space Sci.*, 57, 880–887. [7] G. Neukum, et al., 2004. *ESA Special Publication SP-1240*, 17–35. [8] L. Bandeira, et al. 2012, *Adv. Space Res.*, 49, 64–74.

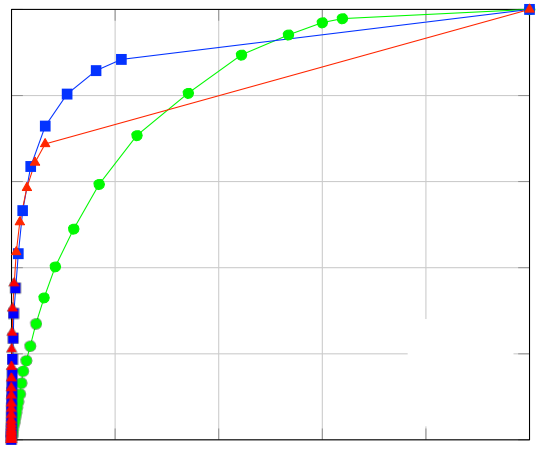

Figure 1. ROC curves for different edge detection parameters. The blue line represents the best response for crater detection.

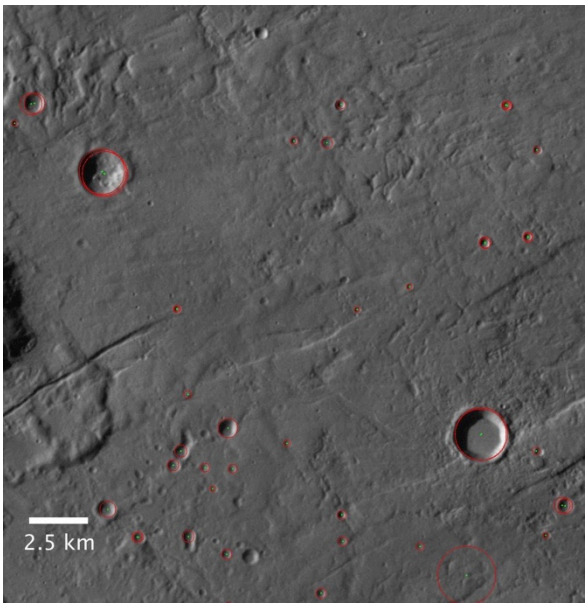

Figure 2. HRSC image with projected detection circles in red.